

**REPUBLIC OF TURKEY
FIRAT UNIVERSITY
GRADUATE SCHOOL OF NATURAL AND
APPLIED SCIENCES**



**A NEW APPROXIMATION TO THE DIFFUSION TENSOR
AT INOSPHERIC F-LAYER'S ALTITUDE IN THE
EQUATORIAL ANOMALY REGION**

Bland Hasan MOHAMMEDNAJEM

Master's Thesis

**Department of Physics
Plasma Physics
Supervisor: Prof. Dr. Ali YEŞİL**

ELAZIĞ-2017

REPUBLIC OF TURKEY
FIRAT UNIVERSITY
GRADUATE SCHOOL OF NATURAL AND APPLIED SCIENCES

**A NEW APPROXIMATION TO THE DIFFUSION TENSOR AT INOSPHERIC
F-LAYER'S ALTITUDE IN THE EQUATORIAL ANOMALY REGION**

Bland Hasan MOHAMMEDNAJEM

(142114112)

Master's Thesis

Date of the thesis submission: 22 December 2016

Date of the thesis defence: 17 October 2017

Supervisor : Prof. Dr. Ali YEŞİL

Referees : Prof. Dr. Osman ÖZCAN

Doç. Dr. İbrahim ÜNAL

November-2017

ACKNOWLEDGMENTS

First of all, I would like to thank Allah for giving me the strength and courage to complete my master's thesis. I would like to express my special thanks to my supervisor, Prof. Dr. Ali YEŞİL. Without him, it would be impossible for me to complete this thesis.

I am indebted to my mother and father, brothers, sisters, my lovely wife and all my friends who encouraged me to complete my master degree with their continuous support during my studies. Finally, I want to say thanks to everyone that help me to prepare a final thesis.

Bland Hasan MOHAMMEDNAJEM
ELAZIĞ-2017

INDEX

	<u>Page No</u>
ACKNOWLEDGMENTS	II
INDEX	III
ABSTRACT	IV
ÖZET	V
LIST of FIGURES	VI
LIST of SYMBOLS	VIII
LIST of ABBREVIATIONS	X
1. INTRODUCTION	1
2. IONOSPHERE REGIONS	6
2.1. D-Region	6
2.2. E-Region	7
2.3. F-Region	7
3. FACTORS INFLUENCING ELECTRON DENSITY	9
3.1. Photo-Chemical Processes	10
3.2. Dynamic Processes	11
3.2.1. Ambipolar Plasma Diffusion	11
3.2.2. Neutral Winds	12
3.2.3. Electromagnetic drag	15
3.2.4. Expansion and contraction of atmosphere	15
3.2.5. Diffusion Between Protonsphere and Ionosphere	16
4. DIFFUSION TENSOR FOR IONOSPHERE PLASMA	18
4.1. Simple Diffusion Equations.....	18
4.2. Diffusion Equations for Anisotropic Ionosphere Plasma	19
5. MATERIAL and METHOD	22
6. RESULTS and DISCUSSION	23
7. CONCLUSION	36
8. REFERENCES	37
CIRRICULUM VITAE	40

ABSTRACT

In this thesis, the classical diffusion tensor (D_0, D_1, D_2) for both steady-state and unsteady-case) for F- region of the ionosphere at the equatorial region is investigated by taking ($\mathbf{B} = B_0 \mathbf{z}$), and by neglecting the neutral winds velocity (U). The calculations were made in the height (280,300,340,390 and 410 km) where the equatorial anomaly was observed predominantly. The magnitudes of the difference of classical diffusion tensor for electrons are $D_0 > D_1 > D_2$ for all seasons with respect to both 12.00LT and 24.00LT at F-region. However, D_1 and D_2 are bigger during nighttime than daytime and show a behavior reverse to the change with latitude of electron density in the magnetic equator. It is possible to say that the behavior of them can be the result of electromagnetic drift and dynamo effect.

Key Words: Diffusion Tensor, Ionospheric Plasma

ÖZET

EKVATORAL ANORMALLIK BÖLGESİ YÜKSEKLİKLERİNDE İYONKÜRENİN F TABAKASINDAKİ DİFÜZYON TENSÖRÜNE YENİ BİR YAKLAŞIM

Bu çalışmada, Klasik difüzyon tensörünün (D_0, D_1, D_2) elamanları nötr rüzgar hızı(U) ihmal edilerek ve Dünyanın manyetik alanı $B=B_0z$, alınarak ekvator bölgesinde etkin yükseklikler olan (280,300,340,390 410 km) kararlı ve kararsız durumda İyonosferin F- bölgesi için çalışılmıştır. Klasik difüzyon katsayılarının büyüklükleri F- bölgesinde hem 12.00 gündüz ve 24.00 gece yerel zamana göre bütün mevsimler için $D_0 > D_1 > D_2$ dir. Ancak, D_1 ve D_2 gündüz gecedan daha büyük değerler almaktadır. Bu manyetik ekvator da electron yoğunluğunun enlemle değişimi ile zıt bir davranış gösterir. Onların bu davranışı elektromanyetik sürüklenme ve dynamo etkisinin bir sonucu olduğu söylenebilir.

Anahtar Kelimeler: Difüzyon Tensörü, İyonosferik Plazma

LIST of FIGURES

	<u>Page No</u>
Figure 1.1. Atmosphere Structure	2
Figure 3.1. Change in densities of neutral atoms and ions in Ionosphere by height.....	9
Figure 3.2. Free electron creation by photo-ionization	10
Figure 3.3. Geometry of vertical velocity of neutral wind.....	13
Figure 3.4. Vertical velocity of neutral wind	13
Figure 4.1. Geometry of magnetic field of Earth (For Northern Hemisphere) ..	19
Figure 6.1. a, b, c: The change of the electron diffusion by local time (March 21, $Z=0$).....	23
Figure 6.2. a, b, c: The change of real parts of the electron diffusion by local time (March 21, $Z\neq 0$).....	24
Figure 6.3. a, b, c: The Change of the imaginary parts of the electron diffusion coefficient by local time (March 21, $Z\neq 0$).....	25
Figure 6.4. a, b, c: The Change of the electron diffusion by local time (June 21, $Z=0$).....	26
Figure 6.5. a, b, c: The change of real parts of the electron diffusion by local time (June 21, $Z\neq 0$).....	27
Figure 6.6. a, b, c: The change of imaginary parts of the electron diffusion by local time (June 21, $Z\neq 0$).....	28
Figure 6.7. a, b, c: The Change of the electron diffusion by local time (September 23, $Z=0$)	29
Figure 6.8 .a, b, c: The Change of real part of electron diffusion coefficient by local time (September 23, $Z\neq 0$)	30
Figure 6.9. a, b, c: The Change of imaginary part of electron diffusion coefficients with local time (September 23, $Z\neq 0$).....	31
Figure 6.10. a,b, c: The Change of electron diffusion coefficients by local time (December 21, $Z=0$).....	32
Figure 6.11. a, b, c: The Change of real part of electron diffusion coefficients by local time (December 21, $Z\neq 0$).....	33

Figure 6.12. a, b, c: The Change of electron diffusion coefficients by local time (December 21, $Z \neq 0$)..... 34



LIST of SYMBOLS

\AA	: Wavelength unit
N	: Electron density
k_b	: Boltzmann constant
m	: Mass
V	: Velocity
V_H	: Vertical velocity of electron
λ	: Wavelength
P	: Pressure
Φ	: Flux
B	: Magnetic field
E	: Electric field
χ	: Zenith angle
D	: Declination angle
e	: Electron load
J	: Current density of electron
ω_p	: Angular plasma frequency of electron
ω_c	: Angular cyclotron (rotation) frequency of electron
∇	: Dell operator
μ_0	: Magnetic permeability
β	: Coefficient of loss (absorption)
q	: Production coefficient
H_p	: Plasma scale height
U_D	: Wind towards east
U_K	: Wind towards north
h	: Planck constant
ν	: Collision frequency
R	: Position vector
ρ	: Fluid mass density

- D** : Diffusion coefficient
T : Temperature
 Γ : Electron flux density



LIST of ABBREVIATIONS

NmF₂ : Maximum density of F₂ Peak

h_mF₂ : Maximum height of F₂ Peak

nm : nanometer

Ne : Electron density

LT : Local time



1. INTRODUCTION

Atmosphere is an air layer enclosing the planet Earth. Atmosphere is where the clouds roam and meteorological events happen and it protects living creatures against external effects. High energy particles from sun are blocked at magnetosphere. While harmful ultraviolet (UV) rays are absorbed during photo-chemical reactions, absorption of X rays and ultraviolet rays by atmosphere causes ionization of atmosphere gases.

Atmosphere is divided into various regions according to temperature, physical events and chemical components. The division of atmosphere according to these attributes is shown in Figure 1.1. It is divided into five regions as troposphere, stratosphere, mesosphere, thermosphere and exosphere by temperature. Into four regions as ozonosphere, ionosphere, heliosphere and protonosphere by chemical components. As for physical attributes, it is divided into three regions as mixed region which under the effect of too complex events at close heights of earth, diffusion region where each gas moves separately under the effect of gravity by its own weight and magnetosphere where the earth's magnetic field take the loaded particles under its hold.

Troposphere is the lowest layer of Atmosphere. It is where the atmospheric events happen most intensely. This layer stretches up to about 10 km height from the surface. Due to variations of water vapor, pressure and temperature, it is not homogeneous. Rays larger than 800 nm wavelength are essentially absorbed by H₂O and CO₂. The highest concentration of gasses found in this layer are oxygen and nitrogen molecules. Weather events such as rain and snow happen in this region.

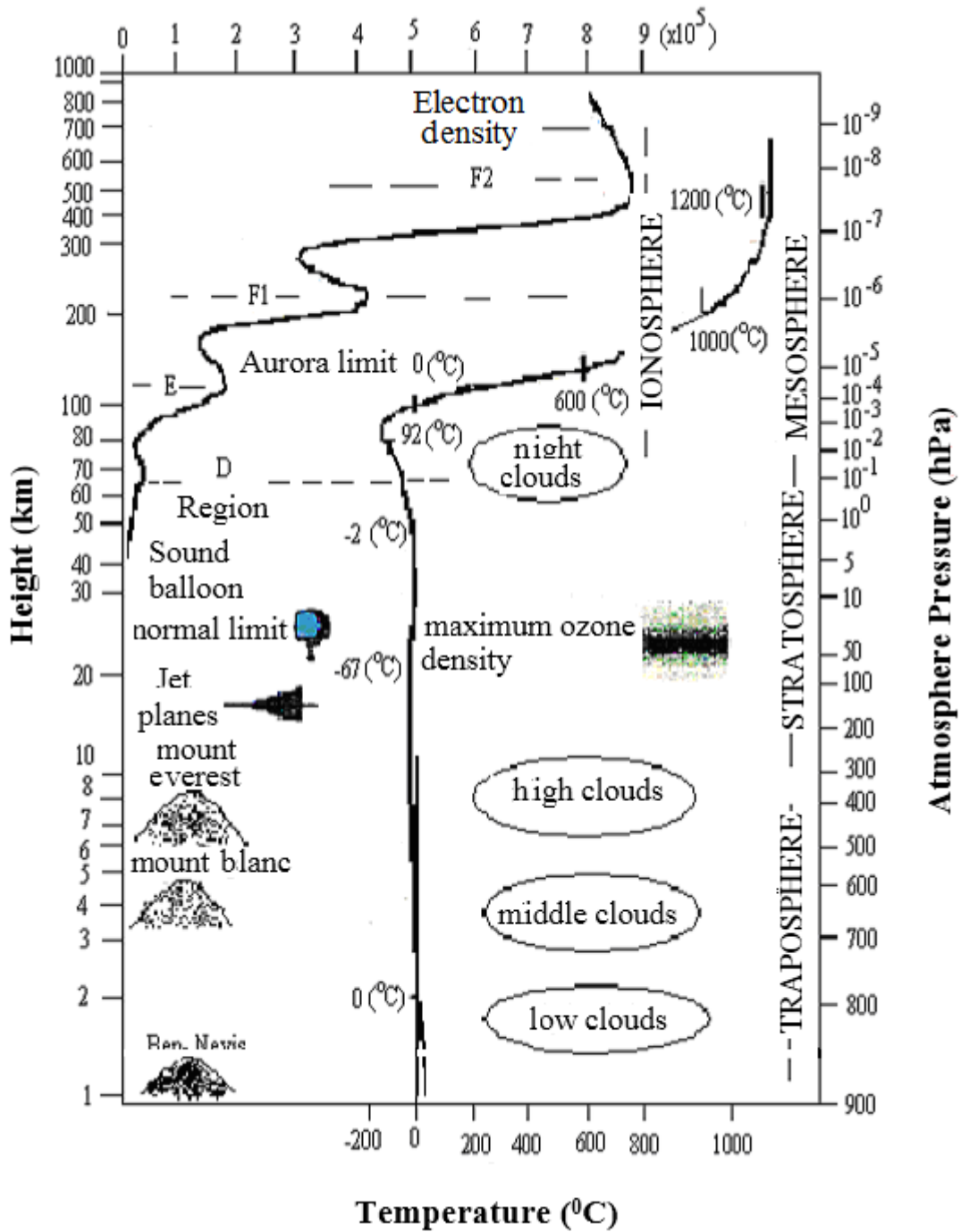


Figure 1.1. Atmosphere Structure [14].

The atmospheric region above 10 km is called Stratosphere. Gases keep their densities about up to 35 km height in this region. Ozone layer is at about 25 km height within stratosphere. Ozone layer was formed by UV rays naturally affecting O_2 molecules. Ozone layer is very important for the living creatures on the Earth. Because this layer absorbs the incoming harmful rays. The region after Stratosphere and stretch

up to 85 km as upper border is called Mesosphere. This region is the coldest region of the Atmosphere. Rays between 175–200 nm wavelength have formed this region by being absorbed by oxygen. Thermosphere is the region above Mesosphere. The main reason of ionization in this region is radiations smaller than 175 nm wavelength. Its temperature at about 500 km height is 1700 °C. The collision between molecules in Exosphere is very low. Ionized particles can be moved in short distances in this region by magnetic field and neutral particles by gravity. The region of Atmosphere formed by Sun rays is called Ionosphere. It consists of usually equal number of free electrons, positive ions and neutral components. Therefore, Ionosphere is the ionized section of Atmosphere and is electrically neutral. Due to this property, Ionosphere is considered a natural plasma. The largest effect in forming of Ionosphere is created by Sun but since the chemical structure and components of each region are different, the rays with different wavelengths coming from the Sun creates regions with different structures. Electron density in Ionosphere changes according to height, latitude, season and local time. Ionosphere starts at about 50 km height from Earth and although the upper border is not certain, it is considered to end at a height where light ions such as He⁺ and H⁺ became dominant to ions such as O⁺. Ionosphere is divided into three regions according to electron density as D, E, F (F1, F2) [1, 2].

In studies made about Atmosphere, the Trans-Atlantic experiment of Marconi in 1901 has provided important steps in this field. As a result of this experiment, the wave passing the Atlantic lead to the result that it can only be reflected from ionized layers due to Earth not being a planar structure. In later researches, the structure, changes, physical processes affecting and shaping its behavior were revealed. Long distance communications are made by reflection and radiation of electromagnetic waves from ionosphere. The most important region in terms of radio communications is F2 region where electron density is highest. The height of this region (hmF2) changes between 200-400 km. The electron density in this region influences the plasma diffusion, neutral winds, thermal movements and electric field drag. The reflection of waves from ionosphere depends on the refractive index of the environment and frequency of the wave. High frequency radio waves requires reflection from upper heights, however when the wave frequency is too high, the wave may pass without reflecting. Also, the

waves are absorbed in the lower layers of ionosphere. This effect is larger for lower frequency waves [1, 2, 3, 4,5].

Ionospheric plasma events could be analyzed using macroscopic momentum transport equations not only by considering the plasma as a multi-constituent fluid but also by treating the plasma as a single conducting fluid. There is force of pressure gradients that are associated with the existence of either density gradients or temperature gradients, or both in ionospheric plasma. This motion of the electrons, induced by pressure gradients, is called diffusion[6]. The diffusion subject has been studied by a lot of authors both theoretically and empirically in the ionosphere plasma [3, 7-13]. Actually, the diffusion studies hold up until the beginning of the 20th century in ionospheric plasma. Mariani, F. obtained diffusion equations including the thermal diffusion theoretically in 1956 after Ferraro's approximations in non-isothermal ionosphere. Fiala, V. (1963) conducted a study which examined the non-potential component of the electric field diffusion of inhomogeneity which drifts due to the motion of the neutral component of the ionospheric plasma or external electric field. The findings of his work showed that when considering the non-potential electric field, it depended weakly on the drift velocity of an inhomogeneity and the parameters related to the ionosphere was omitted for the ambipolar diffusion. The same researcher published a detailed paper on diffusion in anisotropic ionosphere and resolved the momentum and continuity equation by using some approximations and did some corrections in the diffusion equation in 1967. In 2011, Pavlov, A. V. and Pavlova, N. M. showed that the general expression for thermal diffusion and diffusion correction factors in an ion would be simplified by using Grad's 13-moment approximation in multicomponent partially ionized plasma. Besides, Bohm-Type Coefficient of Diffusion was used by Dominguez, H. J. Quantum Mechanical methods in plasma[14]. One of the recent studies on the diffusion subject in the ionospheric plasma is the one which was conducted by Sagir et al., 2014. They suggested a new solution that established a relationship between the electrical conductivity and diffusion equation and applied it to ionospheric plasma for mid-latitudes. The vast majority of authors studied the diffusion coefficients of not only electrons but also minor ions as the frequency independent for mid-latitudes in the ionosphere plasma, and their findings showed that electrons and a

number of minor ions resulted from a temperature gradient in gas or from a relative drift between the major ion gases[23-29].

The equatorial anomaly is an anomaly in the E/M field of the Earth, creating ionization crests about 17° north and south and a trough at the equator itself. When upward drifting ionization loses its momentum it diffuses under gravity along the magnetic field lines to higher latitudes where it causes an increase in the ionization concentration defined as the equatorial anomaly[23-27].

Ionosphere plays a constructive role in radiation of very long and short waves. For very long waves, the bottom region of ionosphere plays the role of conductor. For long and medium waves, the ionosphere acts like a lossy conductor. Especially the long wave radiation is used in submarines for guidance via high attenuation. Very long waves are returned to earth by reflecting from D layer. Thus they move to very long distances between earth and D layer with very low attenuation. Ionosphere acts like a highly lossy environment in day time and low lossy environment at night. This causes the waves to fade out by creating differences in medium and long wave radiation. D layer acts like low lossy environment for short waves both in day time and at night. Thus short waves can be transmitted to much longer distances with high attenuation. If medium and long waves hit D layer, they are faded out by high attenuation due to highly lossy environment [4].

2. IONOSPHERE REGIONS

X and UV (ultraviolet) rays from the Sun forms the most important source of ionization in atmosphere and electron production. These radiations lose their intensity due to absorption as they move in the atmosphere. They are completely absorbed and lose their effectiveness at the height where their intensity falls down to $1/e$. Since ionization would be higher where absorption is high, maximum ionization occurs at this height. Electron production being directly proportional with $\text{Cos}^{1/2}\chi$ (χ zenith angle) was discovered by Chapman. Ionization at about 170 km by heights of the value $1/e$ are made by radiations at 500-600 Å wavelengths. Since the O_2 molecule at around 100 km will be decomposed to O atom, it is seen in high amounts at this height. We can summarize the radiations forming the ionosphere layers as follows:

D Region: 1-10 Å X-radiations and 1216 Å UV

E Region: 10-200 Å X-radiations and 800-1030 Å UV

F Region (Bottom parts of F region): 200-800 Å UV

The region below 80 km where sun rays could not get to is ionized by cosmic rays and solar rays. This region is called C region. [8]

2.1. D-Region

D-region is the poorest region of ionosphere in terms of electron density. Most of the ionization in this region provided by X rays between 1-10 Å and UV radiation with wavelength higher than 1030 Å. Therefore these radiations are an important source for electron production in D-region. Other than these radiations, Lyman- α radiations with wavelengths around 1216 Å go down to D-region and ensure ionization of NO^+ ion. Also, since high energy cosmic rays have high energy, they can only be absorbed after 70 km. The effects of these radiations appear especially at night.

Electron production in D-region depends largely on the effect of Sun. Electron production starts to increase just after the sunrise. The increase in electron density is

inversely proportional to the zenith angle (χ) of Sun. The highest production happens at noon hours. The decrease in electron density starting after noon hours continues until sunrise. Electron density at the height of 85 km at night hours decreases to a level about 10^8 per cubic meter. The existence of electron density at this height at night hours is completely by the effect of cosmic rays. Basic ions in D-region are O_2 , N_2^+ and NO^+ .

2.2. E-Region

Generally, it is accepted that E-region is formed by X rays with wavelengths 10–200 Å and UV rays with wavelengths 800–1026 Å. UV radiations are absorbed completely at 100–120 km's and ionizes the O_2^+ and N_2^+ molecules maximum at 125th km. Since ionization also means electron production, maximum electron density in E-region was also measured at these heights.

In E-region, NO^+ ion is found most. Then, respectively O_2^+ , O^+ and N_2^+ are found mostly according to their ions. Since NO^+ and O_2^+ ions are found in very large amounts compared to O^+ and N_2^+ ions in E region, a large electron loss happens through photo-chemical processes.

Maximum production of electron density in E-region changes as $\cos^{1/2}\chi$ by the zenith angle (χ) of Sun at around 100 km. While the electron density in this region is about $10^{11} / m^3$ level in day times, it decreases to the level of around $10^9 / m^3$ at night hours. The reason of this big change in electron density is the dominance of photo-chemical processes in E-region.

2.3. F-Region

The region after the 150th km of Ionosphere is defined as F region. Along with the upper border not being certain, it is considered as the height where light ions such as H^+ and He^+ are dominant compared to O^+ ion. It is the most important region in terms of radiation of short waves. UV radiations above 200–800 Å are basic sources of

ionization. Sun radiations in this wavelength are mostly absorbed between 160–180 km and form O_2^+ , N_2^+ ions. F region of Ionosphere is divided into two layers as F1 and F2.

F1-region is formed at about the height of 150–180 km, by ionization of UV radiations between wavelengths 200–900 Å. Electron density is maximum between 200–300 km. Besides NO^+ and O_2^+ ions, O^+ and N^+ ions are found secondarily in this region.

F2-region is at about 180–450 km height. It is the region where electron density is maximum. UV radiations with wavelengths between 200–800 Å provide basic ionization. The most important attribute of this region is the role it plays in radio communication. Maximum electron density in this region is seen around between 240–450 km [3]. O^+ is the basic ion in this region. Besides, H^+ , He^+ , N^+ ions can also be found.

Ionosphere plasma consists of free electrons, positive ions and neutral atoms. The most active particles in the plasma are ions.

The F-region maximum electron density (N_mF2) value not depending on only to $\cos^{1/2}\chi$ factor was revealed as a result of measurements. Movement of Ionosphere plasma by winds and photo-chemical processes are effective on this region.

3. FACTORS INFLUENCING ELECTRON DENSITY

While the electron density in Ionosphere is created in one process, it is lost in another process. Also, they may be moved from one region to another through dynamic processes in the atmosphere. Moving procedures are a gain for one region, while a loss for another region. Photo-chemical processes are the most important factor for regions D and E. In F2-region, dynamic processes as well as photo-chemical processes are effective. Therefore it would be correct to divide processes affecting the electron density in F2-region as photo-chemical and dynamic processes. Change in densities of neutral atoms and ions in Ionosphere by height, is shown in Figure 3.1.

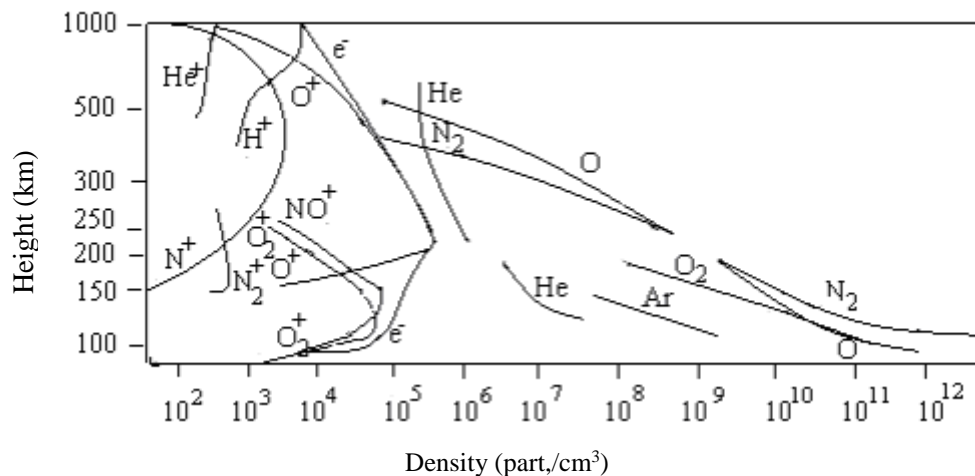


Figure 3.1. Change in densities of neutral atoms and ions in Ionosphere by height [5].

Photo-chemical processes are;

Particle movement

Ionization of X and UV rays

Loss mechanisms, ion-atom exchange, decomposing and reunification processes.

Dynamic processes are;

Plasma ambipolar diffusion

Neutral winds

Electromagnetic drag

Expansion and contraction of atmosphere.

The equation of continuity for change of electron density in time, depending on the production, loss mechanism and movement processes in Ionosphere can be shown as:

$$\frac{\partial N}{\partial t} = q - \beta N - \text{div}(N.V) \quad (3.1)$$

Here, q means production, β loss coefficient, NV dynamic processes [6].

3.1. Photo-Chemical Processes

UV radiation are the source of ionization in F-region. However, X rays also contribute to the ionization. Also, the effects of particle ionization could not be fully measured. The most important gain for F-region, O atom ionizing by means of photo-chemical, is shown in Figure-3.2 schematically [15].

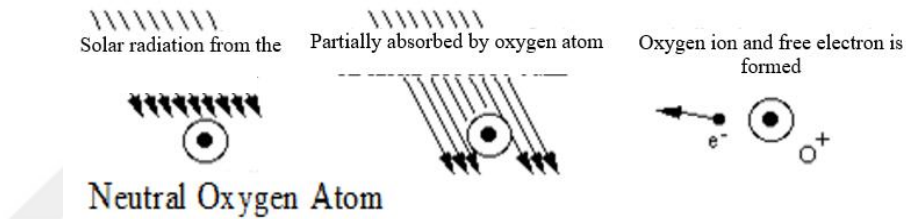


Figure 3.2. Free electron creation by photo-ionization [15].

Radiation coming from the Sun is quite effective on a gas atom or molecule. In the process, part of this radiation is absorbed by atom and a free electron and a positive ion is thusly created.



Thusly ensured. Here, h is Planck constant, ν is incoming radiation frequency. O^+ ion created with 3.2-correlation can combine with O_2 and N_2 molecules as :



O^+ and NO^+ ions created with (3.3) and (3.4) correlations, cause electron loss by combining with electrons in free state [7]. So,



Ionization of N molecule in F region as :



Also ensures electron production. In case of no dynamic process, it is equal to electron loss of about up to 200 km. But, this equality is disrupted during sunrise and sundown. The correlation will increase during sunrise according to 3.2. As for the sundown, the loss is not that much.

3.2. Dynamic Processes

The effects of dynamic processes on electronic density about up to 200 km are low. Up to this height, electron density production and loss processes can be determined. However, after about hmF2 height, the effects of dynamic processes on electron density are more than photo-chemical process.

3.2.1. Ambipolar Plasma Diffusion

Ions and electrons are diffused under partial pressure and gravity effect. This diffusion is prevented due to collision between the gas molecules. Therefore the diffusion speed depends on the density of gasses.

Each gas diffuses according to its own scale height at the heights after F2 peak where diffusion equilibrium is dominant. Since the mass of electron is a lot smaller than mass of ion, scale height is very high. Therefore electrons diffuse by going higher and ions diffuse by staying at lower sections. Electrostatic force between electrons and ions pulls the electrons down and ions up. Thus as the scale height of electrons decrease, scale height of ions increase. When the scale height of electron is twice the scale height of ion, ions and electrons diffuse by same scale height. In the end, ions and electrons

have started to diffuse together with the same velocity. This kind of diffusion is called ambipolar diffusion [8].

Vertical direction change of electron density is a lot larger than horizontal direction. Therefore the diffusion in horizontal direction can be omitted. The diffusion velocity, initially considering the magnetic field of Earth is in vertical direction, is as

$$V_p = -D \left[\frac{1}{N} \frac{dN}{dh} + \frac{1}{2H_p} \right] \quad (3.8)$$

$D=k(T_e+T_i)/m_i v$ here is diffusion constant, $H_p=k(T_e+T_i)/m_i g$ plasma scale height and N is electron density. Then, vertical direction component of V_D velocity becomes [8].

$$W_D = V_p \sin I = -D \left[\frac{1}{N} \frac{\partial N}{\partial h} + \frac{1}{H_p} \right] \sin^2 I \quad (3.9)$$

Influencing the electron diffusion in F2 region is W_D velocity. W_D velocity, which is downward, pushes F2-region down, W_D velocity which is upward, lifts the region up. Also, due to geometry of magnetic field, W_D velocity has the most effect in polar region where the magnetic field is perpendicular to earth's surface [8].

3.2.2. Neutral Winds

Daily heating and cooling caused by Sun rays, usually cause horizontal winds blowing from the warmer part of the earth in day time to cooler part of the earth at night. This wind with horizontal direction flows from high pressure to low due to the difference in pressure caused by the temperature difference of day and night [9].

Despite the winds blowing in horizontal direction, ions and electrons are forced to move along the magnetic field. Projection of horizontal wind along magnetic field is given by [9]:

$$V = U \cos(D - \theta) \cos I \quad (3.10)$$

As for vertical component is

$$W_N = -(U_D \sin D + U_K \cos D) \sin I \cos I \quad (3.11)$$

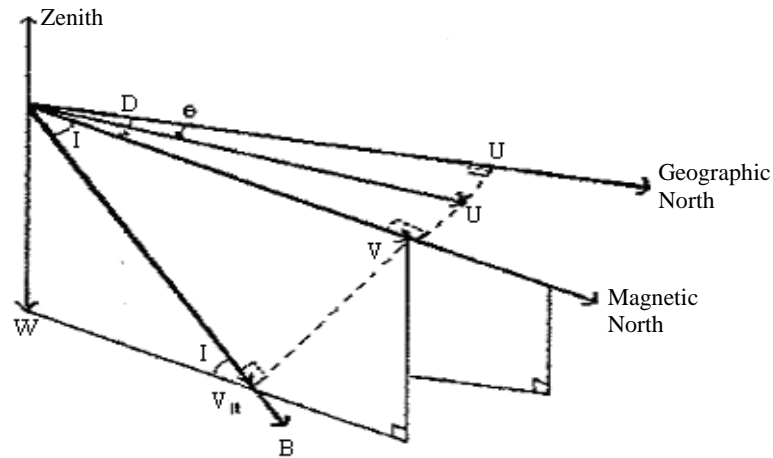


Figure 3.3. Geometry of vertical velocity of neutral wind [9].

In equation 3.12, D is declination, I is magnetic dip, U_D , U_K are winds blowing in east and north direction reciprocally. Vertical velocity geometry of neutral wind is shown in Figure 3.3. Since, with the influence of neutral wind, the curves of daily distribution of electron density look like a bite, this is called "bite-out" [9].

Velocity of the winds change by latitude. Abur-Robb (1969), has found out that the wind velocity has a maximum in ± 45 latitudes and disappear at equator and poles, also at 45° latitude during day times in polar region, despite the wind velocity being low, caused an equatorial anomaly at late hours in the evening. He identified that neutral wind continues (effective) at night in the equatorial F2 region.

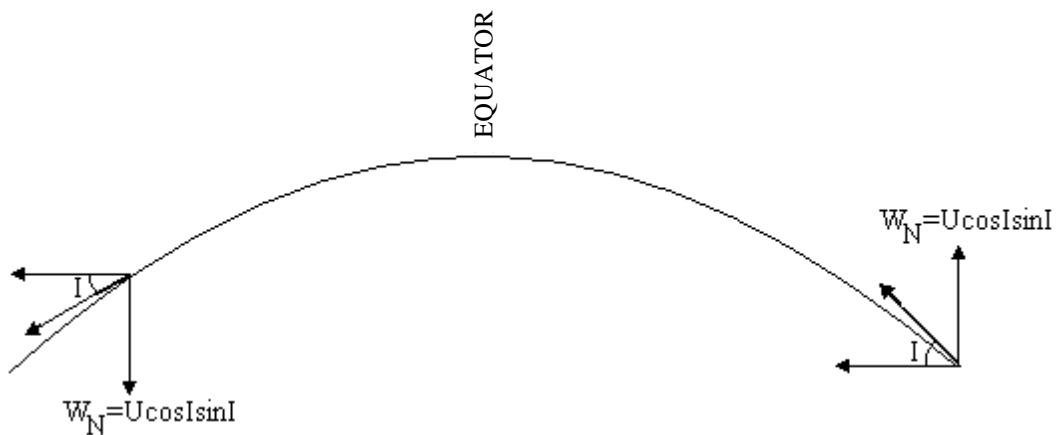


Figure 3.4. Vertical velocity of neutral wind [9].

As can be seen from Figure 3.4, neutral winds move the Ionosphere by carrying up and down. Neutral winds blowing in the direction of equator at night carry a

stationary region to regions where loss is less, upwards. As for the day time, this drag pushes the region to lower regions where loss is more, via total opposite effect. Neutral winds form a "bite-out" in the afternoon during solstice and equinox months in the value of N_mF2 . At night, it is an important factor in existence of Ionosphere. Large values at N_mF2 at night is caused by upwards drag by wind in the equator, during afternoon and evening hours [9].

At night, production stops in F3 region after sundown and losses start. Just before the sundown, density increases and reaches a maximum during evening hours. The decrease in electron density in F2 region during night happen irregularly. This decrease does not continue through the night. Especially in winter, the density fluctuates. In middle latitudes, electron density decreases very slowly in winter months and after midnight in equinoxes and stays close to sunrise with secondary changes (Base level). This base level is around 10^5 cm^{-3} . In high latitudes, neutral winds carry the plasma to regions at night to where loss is less, upwards and cause and increase in electron density. As for the low latitudes, neutral winds together with electromagnetic drag ensure continuity of F2 region at night [9].

In F2 region, electron temperatures being more than ion temperatures can be observed at night as well as in the day. At night, there is no energy source heating up the plasma. Plasma, when cooled off, gives the correlation ($N_m \propto T^{-1/2}$) between electron density with high temperature capacity, electron temperature and electron density [9]. Production stops at night. Therefore the changes in the electron density at night shall be dependent on loss and movement processes. By numerical analysis of the change data depending on the height and local time at night, it is possible to obtain values for loss, diffusion and drag velocity [9]. Loss and diffusion values at fixed height is found considerably smaller at night compared to day. This provides an answer to night anomaly. This difference in loss ratio between the night and the day is due to thermal expansion and contraction causing a huge difference in molecular density at fixed heights. This can also be explained by the upwards drag effect due to neutral winds. However, these mechanism do not completely stop the losses in electron density. Risbeth and Garriot (1967) have found out that F2 peak (h_mF2) is larger at night compared to day.

Other than these, the process with an important effect in the increase of electron density at night is the downward flow of H^+ ion at night. Since the density of O^+ ion at night is lesser compared to day time H^+ layer (protonosphere) goes down [9].

3.2.3. Electromagnetic drag

Due to the heating effect of Sun and gravitational pull of Moon and Sun, the air struggles to move between the magnetic lines of Earth. This movement causes an electric field as much as $\mathbf{E} = \mathbf{U} \times \mathbf{B}$. The flow caused by this electrical field occurs disconcertedly and causes a new electrostatic field by influencing polarization of loads. The E electric field, which is perpendicular to B magnetic field, moves the particles perpendicular to magnetic field. This velocity is given by

$$V_e = \frac{\mathbf{E} \times \mathbf{B}}{B^2} \quad (3.12)$$

The vertical component of this velocity is as [9]:

$$W_e = \frac{E_y}{B} \cos I \quad (3.13)$$

Here, while the day time electric field is towards east W_e velocity is upwards and lifts F2-region up; while at night the direction of electric field is towards west and the direction of W_e velocity is downwards. Therefore the electromagnetic drag which is downwards at night in middle latitudes causes very small loss in electron density [9].

3.2.4. Expansion and contraction of atmosphere

T_e and T_i temperatures sustain sudden changes during sunrise and sundown. These changes in temperature causes expansion and contraction of atmosphere.

Mathematical expression of physical processes in F-region of Ionosphere is determined by (3.1)-correlation. The expansion and contraction of the atmosphere also have a contribution on the change due to movement term $\text{div}(NV)$ in the expression. Accordingly takes the form of:

$$\text{div}(\mathbf{N}\cdot\mathbf{V}) = \frac{\partial}{\partial h}(\mathbf{N}V_h) \quad (3.14)$$

Here, h shows vertical direction and V_h the velocity of electron in vertical direction. The correlation for upper Ionosphere at night hours is $q=0$ in (3.1) equation and L is approximately zero. Continuity correlation under these conditions can be written as [5].

$$\frac{\partial N}{\partial t} = \frac{\partial \Phi}{\partial h} \quad (3.15)$$

$\Phi = -\mathbf{N}V_h$ here is the electron flux [5].

As for the velocity expression here is

$$\mathbf{V}_h = \frac{dH}{dT} + \frac{H}{N} \frac{dN}{dt} \quad (3.16)$$

According to this expression, electron density and the changes in scale height causes a velocity to occur in the vertical direction. During sunrise and sundown, sudden changes in electron and ion temperatures cause sudden changes in scale height. As a result of this, the vertical velocity increases. During sunrise, the direction of the velocity is up and during sundown is down [5].

3.2.5. Diffusion Between Protonsphere and Ionosphere

The density of oxygen ions above F2 region decreases exponentially with H scale height. This decrease can be shown as $N(\text{O}^+) \approx e^{-\frac{h}{H}}$ [5]. But however, the density of H^+ ion increases with height. The region where H^+ is dominant in atmosphere is defined as protonsphere. Production or destruction of H^+ ion is actualized alternatively. So,



The density of these ions supervises the electron density of Ionosphere. Since the density of O^+ ion at night is less than day times, it lowers the H^+ layer at night.

Starting to decrease by sundown, electron density starts to increase at about 18.00-23.00 LT with the H^+ ion flux from protonosphere [5].



4. DIFFUSION TENSOR FOR IONOSPHERE PLASMA

If there are no external influence for the movement of particles from one place to other in Ionosphere plasma, it originates from pressure-gradient (∇P). This force is created towards removing the inhomogeneity occurring in any part of the plasma [8].

The equations related to Ionosphere plasma obtained by taking the situations mentioned above with the help of relevant literature into consideration are as follows.

4.1. Simple Diffusion Equations

Considering the deviations from the equilibrium formed by the inhomogeneity in the density are very small and these disequilibrium's of density are of the first level, velocity distribution is considered approximately isotropic. In that case, density can be defined as below.

$$n_{\alpha}(\mathbf{R}, t) = n_{0\alpha} + n(\mathbf{R}, t) \quad (4.1)$$

Here, $\alpha=e,i$ is for (electron-ion). $n_{0\alpha}$: density at equilibrium and $n(\mathbf{R},t)$: deviation amount of density from equilibrium. \mathbf{R} : position vector. If the Ionosphere plasma is considered an ideal fluid, pressure expression for ion is written as

$$P_{\alpha}(\mathbf{R}, t) = k_b T_{\alpha} n_{\alpha}(\mathbf{R}, t) \quad (4.2)$$

From gas approach. On the condition of $n(\mathbf{R},t) \ll n_0$, if Ionosphere plasma is considered a fluid, both the fluid equations (continuity-momentum) and equations valid for loaded particles can be used due to being electrically loaded. From here, according to continuity equation,

$$\frac{\partial \rho_{\alpha}}{\partial t} + \nabla \cdot (\rho_{\alpha} \mathbf{U}_{\alpha}) = 0 \quad (4.3)$$

Here, \mathbf{U}_{α} is the average velocity of α type fluid and $\rho_{\alpha} = m_{\alpha} n_{\alpha}$ is mass density of α type fluid. If (4.1) equation is used in (4.3) equation;

$$\frac{\partial n_{\alpha}}{\partial t} + n_{0\alpha} (\nabla \cdot \mathbf{U}_{\alpha}) = 0 \quad (4.4)$$

is obtained. If $\mathbf{E}=0$ and $\mathbf{B}=0$, momentum equation for the fluid can be written as

$$\frac{\partial \mathbf{U}_\alpha}{\partial t} + \mathbf{U}_\alpha \cdot \nabla \mathbf{U}_\alpha = -\frac{1}{\rho_\alpha} \nabla P_\alpha - \nu \mathbf{U}_\alpha \quad (4.5)$$

Here ν_α : is the collision frequency of α type particles and (electron-ion, neutral) inside the plasma. If (4.1-2) equation is used in (4.4) equation,

$$\frac{\partial \mathbf{U}_\alpha}{\partial t} = \frac{k_b T_\alpha}{n_{0\alpha} m_\alpha} \nabla n_\alpha(\mathbf{R}, t) - \nu_\alpha \mathbf{U}_\alpha \quad (4.6)$$

Is obtained. When (4.3,4.5) equations are used together, it becomes

$$\frac{\partial n_\alpha}{\partial t} = \frac{k_b T_\alpha}{m_\alpha \nu_\alpha} \nabla^2 n_\alpha(\mathbf{R}, t) - \frac{1}{\nu_\alpha} \frac{\partial^2 n_\alpha}{\partial t^2} \quad (4.7)$$

Here, it is

$$D_\alpha = \frac{k_b T_\alpha}{m_\alpha \nu_\alpha} \quad (4.8)$$

(4.7) equation is known as diffusion coefficient of α type ion.

4.2. Diffusion Equations for Anisotropic Ionosphere Plasma

If $\mathbf{B} \neq 0$, then the environment is called as anisotropic. Since the magnetic field is different than zero in Ionosphere plasma, Ionosphere plasma is anisotropic. If the real geometry of the magnetic field of Earth is used, it becomes three dimensional according to Figure 4.1.

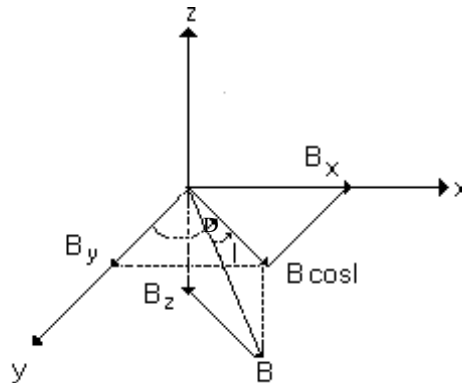


Figure.4.1. Geometry of magnetic field of Earth (For Northern Hemisphere) [2].

Here, $B_x = B \cos I \sin d$, $B_y = B \cos I \cos d$ and $B_z = -B \sin I$. I is magnetic dip and D is magnetic declination angle. Other rotations to be used in this study are as follows:

ω_c : Electron Cyclotron (rotation) frequency. These frequencies are given as

$$\omega_{cx} = \frac{eB_x}{m}, \quad \omega_{cy} = \frac{eB_y}{m} \quad \text{and} \quad \omega_{cz} = \frac{eB_z}{m}$$

depending on the plasma parameters.

Flux density from correlation (4.4) is obtained as:

$$\Gamma + \frac{n_\alpha}{v_\alpha} \frac{D\mathbf{U}}{Dt} = \mu_\alpha (\Gamma \times \mathbf{B} + n_\alpha \mathbf{E}) - D_\alpha \nabla n_\alpha \quad (4.9)$$

Here, $\mu_\alpha = \frac{q_\alpha}{m_\alpha v_\alpha}$ is mobility of the loaded particle. Γ : electron flux density

From the resolving of this expression, if the flux density is written as

$$\Gamma = n_\alpha \mathbf{U} \quad (4.10)$$

diffusion tensor

$$D \nabla n = \mu (\Gamma \times \mathbf{B}) \quad (4.11)$$

From here, the diffusion tensor;

$$D = \begin{bmatrix} D_1 & D_2 & 0 \\ -D_2 & D_1 & 0 \\ 0 & 0 & D_0 \end{bmatrix} \quad (4.12)$$

where (for steady-state case; $\omega=0$), $D_0 = \frac{k_b T}{mv}$, $D_1 = \frac{v^2}{v^2 + \omega_c^2} D_0$ and $D_2 = \frac{v \omega_c}{v^2 + \omega_c^2} D_0$

For unsteady case; $\omega \neq 0$; the elements of diffusion tensor

$$D_0 = \frac{k_b T}{m(v - i\omega)}, \quad D_1 = \frac{(v - i\omega)^2}{(v - i\omega)^2 + \omega_c^2} D_0, \quad D_2 = \frac{(v - i\omega) \omega_c}{(v - i\omega)^2 + \omega_c^2} D_0$$

The differences of diffusion coefficients are obtained by;

$$\Delta D_0 = -\frac{k_b T Z^2}{mv(1+Z^2)} + i\frac{k_b T Z}{mv(1+Z^2)} = \Delta D_{0R} + i\Delta D_{0I} \quad (4.13)$$

$$\Delta D_1 = \left(\frac{k_b T}{mv}\right) \left[\frac{(1+Y^2+Z^2)}{(1+Y^2-Z^2)^2+4Z^2} - \frac{1}{1+Y^2} \right] + i\left(\frac{k_b T}{mv}\right) \left[\frac{2Z-(1+Y^2-Z^2)Z}{(1+Y^2-Z^2)^2+4Z^2} \right] = \Delta D_{1R} + i\Delta D_{1I} \quad (4.14)$$

$$\Delta D_2 = \left(\frac{k_b T}{mv}\right) \left[\frac{Y(1+Y^2-Z^2)}{(1+Y^2-Z^2)^2+4Z^2} - \frac{Y}{1+Y^2} \right] + i\left(\frac{k_b T}{mv}\right) \left[\frac{2YZ}{(1+Y^2-Z^2)^2+4Z^2} \right] = \Delta D_{2R} + i\Delta D_{2I} \quad (4.15)$$

In which;

$Y = \frac{\omega_c}{\omega}$ and $Z = \frac{v}{\omega}$ Here, R refers to the real part, I refers to the imaginary part, k_b refers to the Boltzmann constant, T refers to the Electron Temperature, m refers to the electron mass.

5. MATERIAL and METHOD

The general system of transport equations is applied to the low-latitude for ionosphere F2 region. The restriction to this region of the ionosphere enables us to make several simplifying assumptions that significantly reduce the general system of transport equations. It is fully ionized plasma composed of two major ions, electrons, and a number of minors [1,2,4,6,16]. There are various theories explaining equatorial anomaly. The most important one is Martin's theory dragged upwards by diffusion of plasma. Besides, in this theory, the equatorial anomaly extends on both sides of the magnetic equator between 30°S-30°N latitudes [3]. Therefore, this study examined these latitudes.

The difference ($\Delta D = D_{\omega \neq 0} - D_{\omega = 0}$) of the classical diffusion tensor (D_0 , D_1 and D_2 for both steady and unsteady-case) at the equatorial F2-region of ionosphere plasma was examined seasonally (both equinox (March 21 and September 23) and during the solstice (June 21 and December 21) by taking ($B = B_0 z$) the geometry of Earth's magnetic field for local time (LT) 12.00 and 24.00. The examination was made in the elevation (280, 300, 340, 390 and 410 km) where the equatorial anomaly was observed [17-29]. The results were obtained for I (dip angle)=55.6°, d (Declination)=30°, $R=159$ by using Eqs. (4.12-13). The ionospheric parameters used for calculations were obtained using the IRI (International Reference Ionosphere) model.

The difference of the classical diffusion tensor has a complex mathematical structure as $\omega \neq 0$. It is possible to say that the imaginary part of the difference of diffusion coefficients related to slowing of the average electrons and ions velocity directly depends on the electrons' or ions' mobility. We calculated the magnitude of the tensor elements of the diffusion difference in the accepted conditions and investigated in different seasons (on both equinox and solstice days)

6. RESULTS and DISCUSSION

The seasonal change of electron diffusion coefficient with local time in F region of Ionosphere is given for 240, 280, 340, 390 and 410Km altitudes in Figure 6. 1. a, b, c. The tensor element (D_2) of the electron diffusion coefficient (eq.4.12) takes maximum value at approximately 09.00 LT and 17.00 LT for figures at $Z=0$ in March 21 for 1990 year. But D_1 has maximum value between 10.00LT a.m. -20.00 LT p.m. except 240-280 Km altitudes. D_0 for $Z=0$ has considerably values with respect to local time especially at around 7.00 LT a.m. for March21 in the selected every altitudes. D_0 for this clock has been doing a sharp peak around 7.00 LT a.m. But despite upwards and downwards, the magnitude of it decreases between 10.00 LT a.m.- 20:00LT p.m.

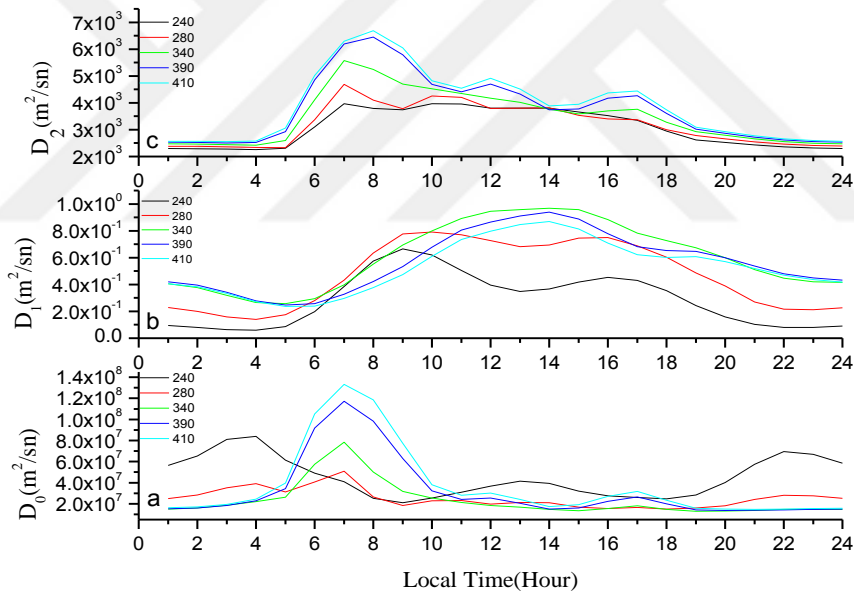


Figure 6.1. a, b, c: The change of the electron diffusion by local time (March 21, $Z=0$)

The change of the real part of the electron diffusion coefficient with local time in F region of Ionosphere is given “eqs.4.13-4.15” in Figure 6. 2. a, b, c.($Z \neq 0$) for 240, 280, 340, 390 and 410Km altitudes for March 21 at the same year. According to these figures, the real parts of the electron diffusion coefficient takes maximum value at approximately 09.00 LT and 17.00 LT for figures at $Z \neq 0$ in March 21 in general. But if $(Z \neq 0)$, D_0 , D_1 and D_2 are bigger than $Z=0$ in march21 for all of the considered altitudes. The real parts of electron diffusion coefficient in the F region of Ionosphere take approximately a value of (10^4) for figure (a) $D_{0R}(m^2/sn)$ and (10^{13}) for figure (b) $D_{1R}(m^2/sn)$ so tensor elements of electron diffusion coefficient in the F region of Ionosphere take approximately a value of (10^4) for figure (c) $D_{2R}(m^2/sn)$.

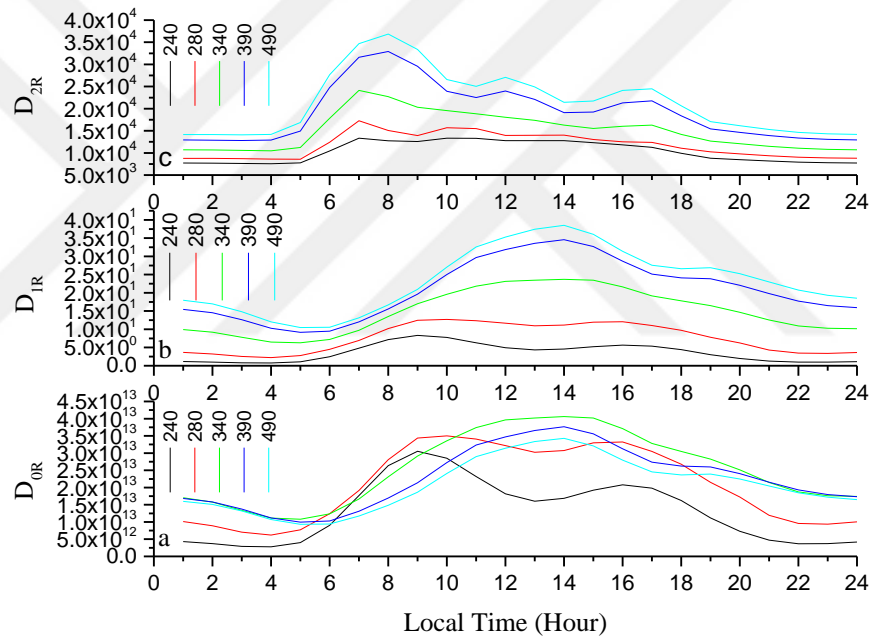


Figure 6.2. a, b, c: The change of real parts of the electron diffusion by local time (March 21, $Z \neq 0$)

According to Figure 6.3. a, b, c.; the change of the imaginary parts of the electron diffusion coefficient with local time in F region of Ionosphere is given for effective altitudes “240, 280, 340, 390 and 410Km” in Eqs.4.13-15, the imaginary parts (D_{0i}, D_{1i}) of the basic tensor elements of the electron diffusion coefficient show similar change as trend and take maximum values at approximately 08.00 LT a.m. and 17.00 LT p.m. for in March 21. Other hand, D_{2i} is to show a different behavior with local time for march21. It takes maximum values between 100LT a.m- 17.00 LT p.m. except for down altitudes (240, 280 Km). Imaginary parts of the electron diffusion coefficient show a different behavior compared to some altitudes. These coefficients suddenly drop at approximately 13.00LT. The basic elements of the electron diffusion coefficient in the F region of Ionosphere take approximately a value of (10^{17}) for figure (a) D_{0i} (m^2/sn) and (10^4) for figure (b) D_{1i} (m^2/sn) so the electron diffusion coefficient in the F region of Ionosphere take approximately a value of (10^1) for figure (c) D_{2i} (m^2/sn). Moreover, they are $D_{0i} > D_{1i} > D_{2i}$ as magnitude. D_{0i} has the biggest value in them.

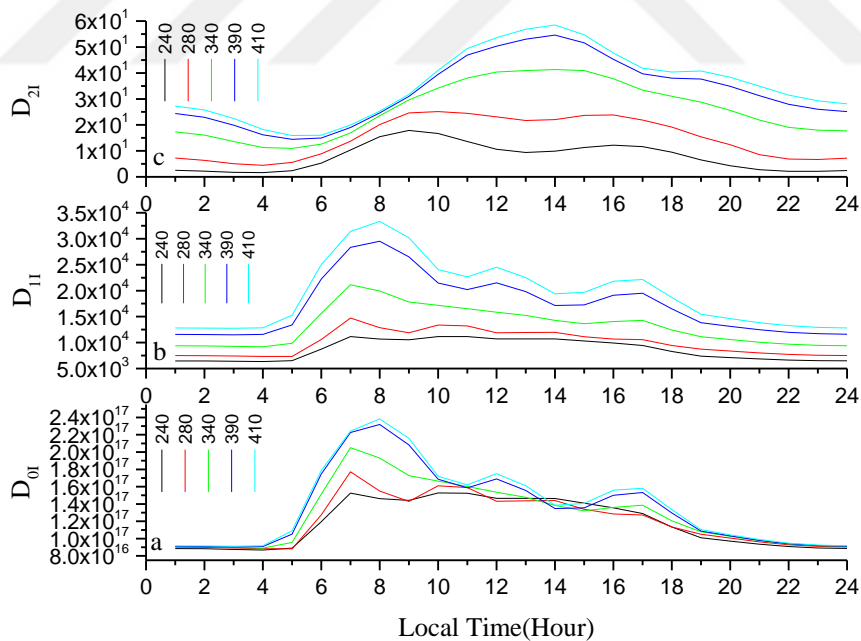


Figure 6.3. a, b, c: The Change of the imaginary parts of the electron diffusion coefficient by local time (March 21, $Z \neq 0$)

The change of the electron diffusion coefficients with local time in F region of Ionosphere has been showing for the selected altitudes “240, 280, 340, 390 and 410Km” in Figure 6.4. a, b, c at June 21 (Z=0). D_0 shows a complex behavior with local time in fig.4a. According to these figure, It is similar to each other as trend with altitude except for 240,280 km altitudes. D_0 takes the biggest value at 7.00 LT a.m. while taking the smallest value at 240,280 km altitudes. After this time, there is sharp upwards and downwards in its value and seriously decreases as magnitude. D_2 is shown similar change with D_0 as trend but D_2 is very smaller than D_0 as magnitude with respect to Fig.4. Most remarkable change is to show D_1 as different from other diffusion coefficients in Fig6.4.b. with respect to the accepted altitudes especially for 340,390 and 410 km altitudes. So, It takes minimum values for these altitudes at around 7.00 LT a.m. for June 21 month. They are D_0 , D_2 , D_1 as magnitude respectively for June 21 month.

The electron diffusion coefficients in the F region of Ionosphere take approximately a value of (10^8) for figure (a) $D_0(m^2/sn)$ and (10^{-1}) for figure (b) $D_1(m^2/sn)$ so tensor elements of electron diffusion coefficient in the F region of Ionosphere take approximately a value of (10^3) for figure (c) $D_2(m^2/sn)$.

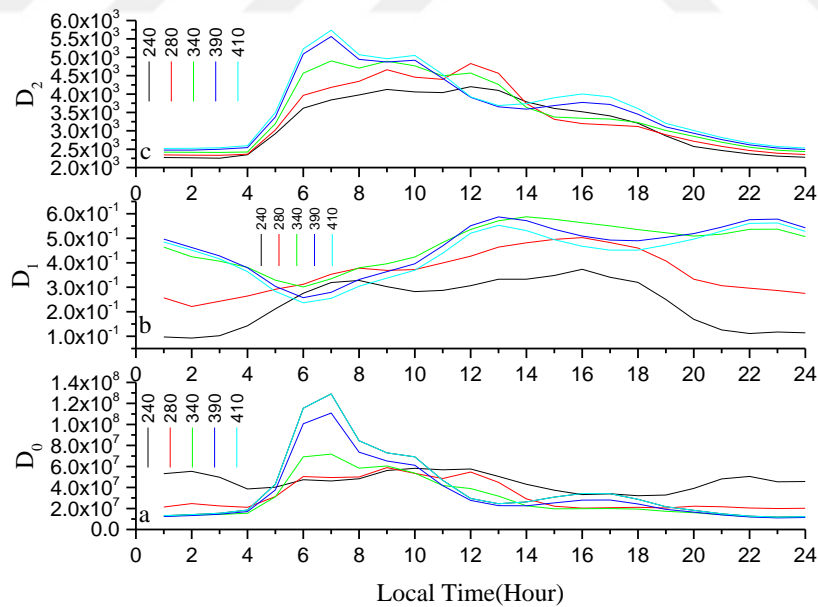


Figure 6.4. a, b, c: The Change of the electron diffusion by local time (June 21, Z=0)

The change of the real part of the electron diffusion coefficients with local time in F region of Ionosphere has been showing for the selected altitudes “240, 280, 340, 390 and 410Km” in Figure 6.5. a, b, c at June21 ($Z \neq 0$). D_{0R} takes the biggest values with respect to other tensor elements and is different as trend and complex for every season. The change of D_{1R} at around at 6.00 LT a.m. sharply decreases for 240,280 and 340 Km and increases for 390,410 Km altitudes. D_{2R} increases between 6.00LT a.m.-12.00 LT all the selected altitudes. The tensor elements of electron diffusion coefficient show a different behavior compared to other seasons. For all seasons, tensor elements of electron diffusion coefficient in the F region of Ionosphere take approximately a value of (10^1) for figure (a) $D_{0R}(m^2/sn)$ and (10^{13}) for figure (b) $D_{1R}(m^2/sn)$ so tensor elements of electron diffusion coefficient in the F region of Ionosphere take approximately a value of (10^4) for figure (c) $D_{2R}(m^2/sn)$.

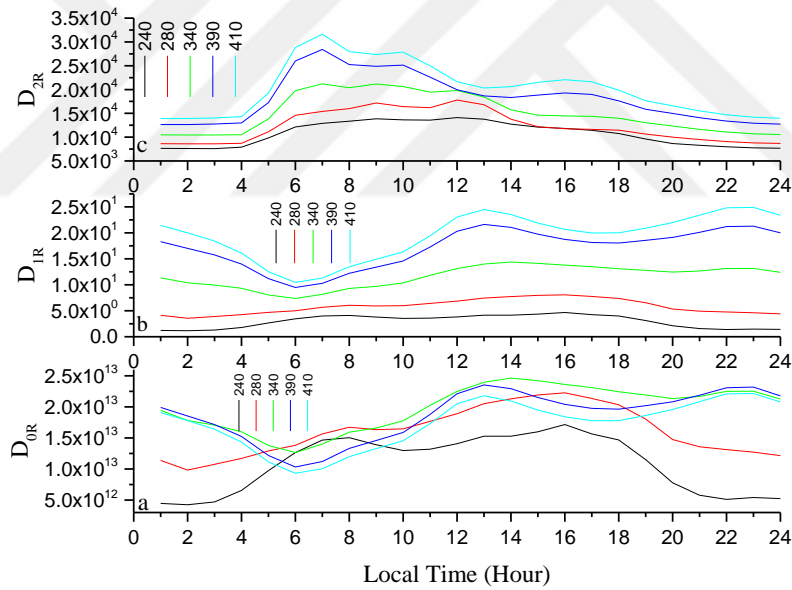


Figure 6.5. a, b, c: The change of real parts of the electron diffusion by local time (June 21, $Z \neq 0$)

The change of the imaginary part of the electron diffusion coefficients with local time in F region of Ionosphere has been showing for the selected altitudes “240, 280, 340, 390 and 410Km” in Figure 6.6. a, b, c at June 21 ($Z \neq 0$). The tensor elements of fig.6.6.a,b, c. is similar to fig.6.5.a,b, c for accepted conditions but the values of the imaginary parts of the electron diffusion coefficients are bigger than real parts for all seasons and altitudes. D_{0I} and D_{1I} are very similar to change of electron density with respect to local time. D_{2I} is different than other tensor elements as trend with local time.

For all seasons, tensor elements of electron diffusion coefficient in the F region of Ionosphere take approximately a value of (10^{17}) for figure (a) $D_{0I}(m^2/sn)$ and (10^4) for figure (b) $D_{1I}(m^2/sn)$ so tensor elements of electron diffusion coefficient in the F region of Ionosphere take approximately a value of (10^1) for figure (c) $D_{2I}(m^2/sn)$.

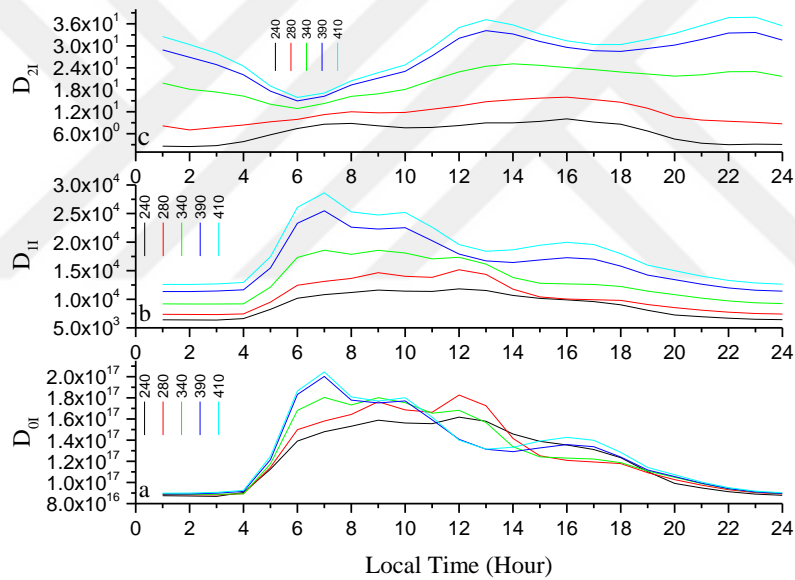


Figure 6.6. a, b, c: The change of imaginary parts of the electron diffusion by local time (June 21, $Z \neq 0$)

The change of the electron diffusion coefficients with local time in F region of Ionosphere has been showing for the selected altitudes “240, 280, 340, 390 and 410Km” in Figure 6.7. a, b, c. at June21 (Z=0). For the considered conditions, the values of tensor elements are $D_0 > D_2 > D_1$ respectively. D_0 takes the biggest values with local time and the change of its is parallel with electron density in ionospheric F- region like D_2 but D_1 is exactly different from D_0 and D_2 as trend.

The tensor elements of electron diffusion coefficient show a different behavior compared to other seasons. For all seasons, tensor elements of electron diffusion coefficient in the F region of Ionosphere take approximately a value of (10^{-1}) for figure (a) $D_0(m^2/sn)$ and (10^8) for figure (b) $D_1(m^2/sn)$ so tensor elements of electron diffusion coefficient in the F region of Ionosphere take approximately a value of (10^3) for figure (c) $D_2(m^2/sn)$.

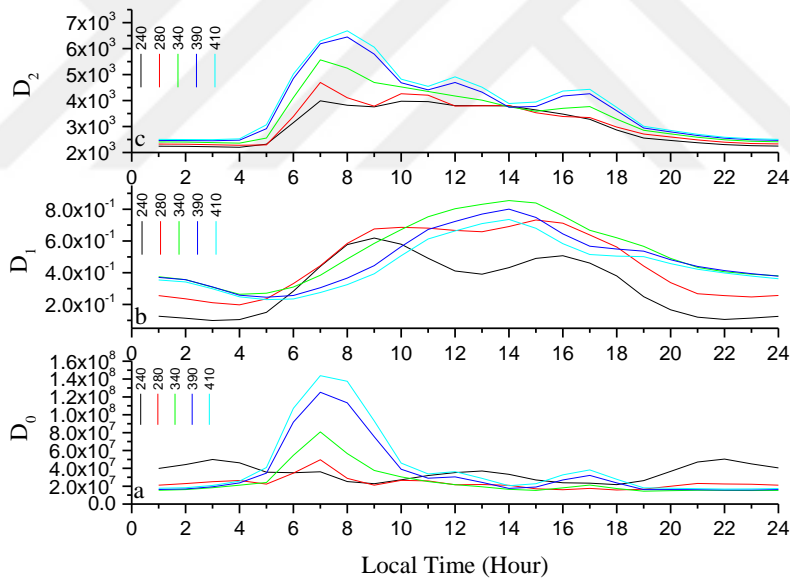


Figure 6.7. a, b, c: The Change of the electron diffusion by local time (September 23,Z=0)

The change of real part of electron diffusion coefficient with local time in the ionospheric F region at autumn equinox at $z \neq 0$ position in the Figure 6.8. a, b, c. is seen. According to these figures, electron diffusion coefficient (240, 280, 340, 390 and 410 km)- D_{2R} -takes maximum value at approximately 07.00 LT(obtained for 240, 280, 340 km altitudes) and 08.00 LT (obtained for 390 and 410 km altitudes) while It take its minimum values approximately 05.00 LT. D_{1R} -takes maximum value at approximately 15.00 LT(obtained for 240, 280 km altitudes) and 04.00 LT (obtained for 340, 390 and 410 km altitudes) while It take its minimum values approximately 05.00 LT. The coefficient obtained for an any altitude are not cut to be obtained the others altitudes both D_{1R} and D_{2R} while this is not true for the D_{0R} .

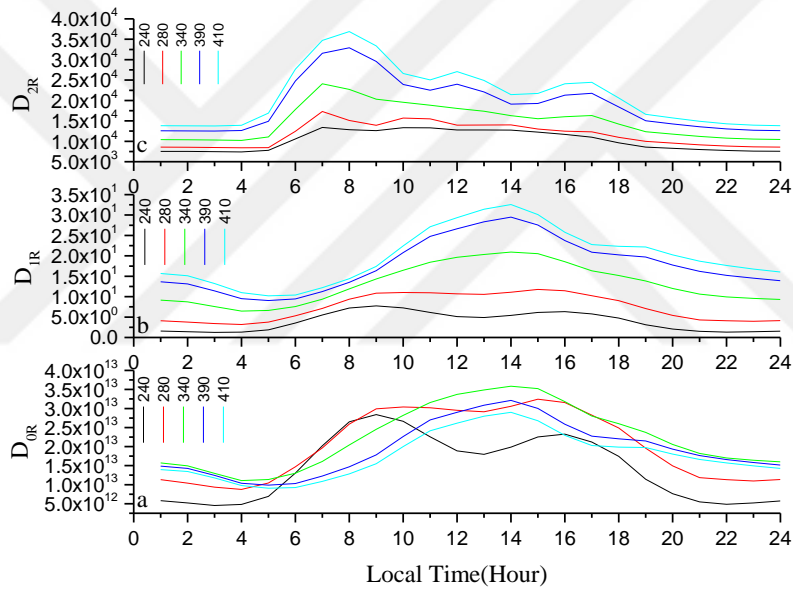


Figure 6.8 .a, b, c: The Change of real part of electron diffusion coefficient by local time (September 23, $Z \neq 0$)

Figure 6.9.a, b, c. Shows the change of imaginary part electron diffusion coefficient with local time in the ionospheric F region at position $z \neq 0$ on September 23. Tensor elements (D_{0I} , D_{1I} and D_{2I}) obtained for 240, 280, 340, 390 and 410 km altitudes. D_{2I} tensor elements takes maximum value at approximately 14.00 LT except it's for 240 km altitude while it take its minimum value approximately at 05.00 LT. D_{0I} and D_{1I} coefficients take its maximum values approximately at 07.00-08.00 LT. Then they are behavior as damped sinusoidal wave.

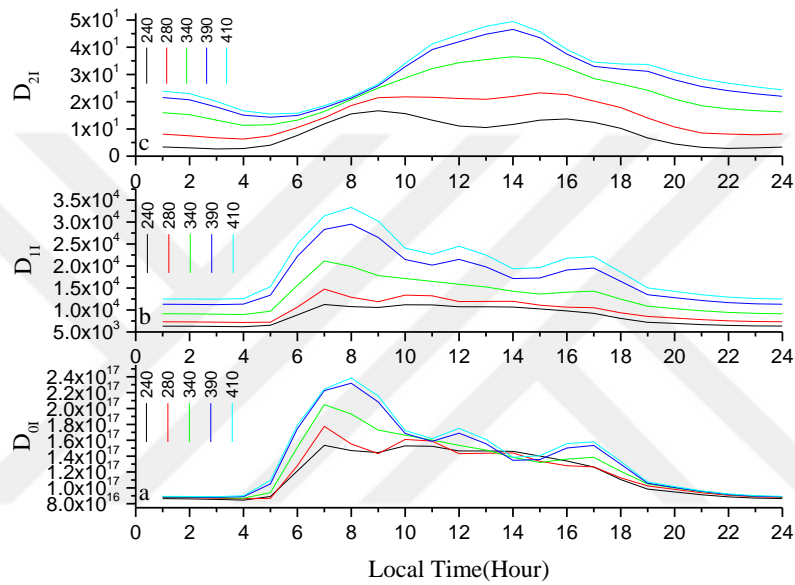


Figure 6.9. a, b, c: The Change of imaginary part of electron diffusion coefficients with local time (September 23, $Z \neq 0$)

The change of electron diffusion coefficient with local time in the ionospheric F region at position $z=0$ on December 21 is seen in the Figure 6.10. a, b, c. tensor elements of electron diffusion coefficient obtained for 240, 280, 340, 390 and 410 km altitude. D_2 elements of electron diffusion coefficient takes maximum value at approximately 10.00 LT and 16.00 LT while it (except for 240 km and 280 km altitude values) suddenly drop at approximately 13.00 LT. D_2 elements takes its minimum values between 20.00 LT and 04. 00 LT. D_1 elements of electron diffusion coefficient takes maximum value at approximately 10.00 LT for 240 and 280 km and 13.30 LT for 340, 390 and 410 km while it takes at 05.00 LT its minimum values for all altitudes. The situation in D_0 is quite different. D_0 coefficient takes its maximum values approximately at 05.00-06.00 LT. Then D_0 is behavior as damped sinusoidal wave. For all seasons, tensor elements of electron diffusion coefficient, D_0 , D_1 , and D_2 take approximately a value of 10^8 , 10^{-1} , and 10^3 (m^2/sn) in order.

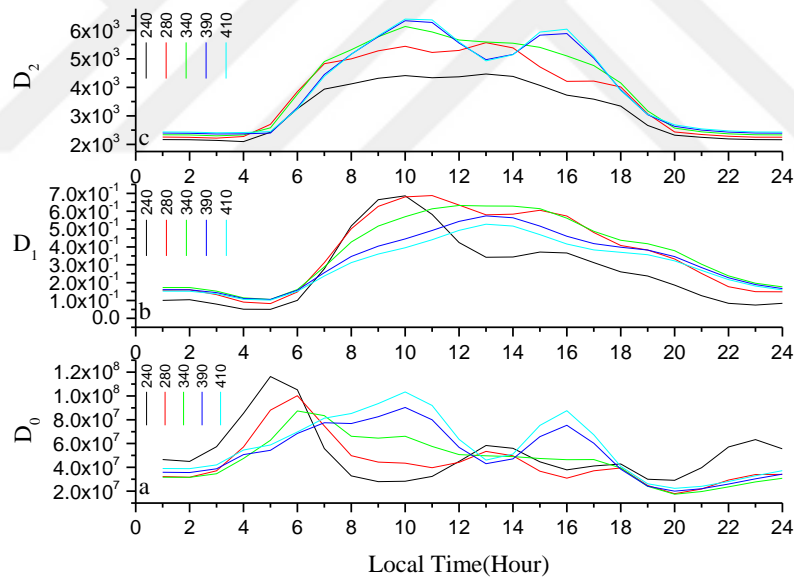


Figure 6.10. a,b, c: The Change of electron diffusion coefficients by local time (December 21, $Z=0$)

Figure 6.11. a, b, c. The change of real part of electron diffusion coefficient in the ionospheric F region with local time at position of $z \neq 0$, on December 21 is seen. According to these figures, tensor elements of electron diffusion coefficient for 240, 280, 340, 390 and 410 km altitudes show different behavior compared to other seasons. The tensor elements, D_{0R} , D_{1R} and, D_{2R} , for at $z \neq 0$ position takes maximum value at approximately 09.00 LT and 15.00 LT (except at 240 km), 09.00 LT and 13.00 LT (except at 240 and 280 km), and 10.00 LT and 16.00 LT, respectively. D_{2R} tensor elements suddenly drop at approximately 13.00 LT. For all seasons, tensor elements of real part of electron diffusion coefficient in the ionospheric F region take approximately a value of (10^{13}) for $D_{0R}(m^2/sn)$ while the elements take approximately a value of (10^4) order for $D_{2R}(m^2/sn)$ and (10^1) order for $D_{1R}(m^2/sn)$.

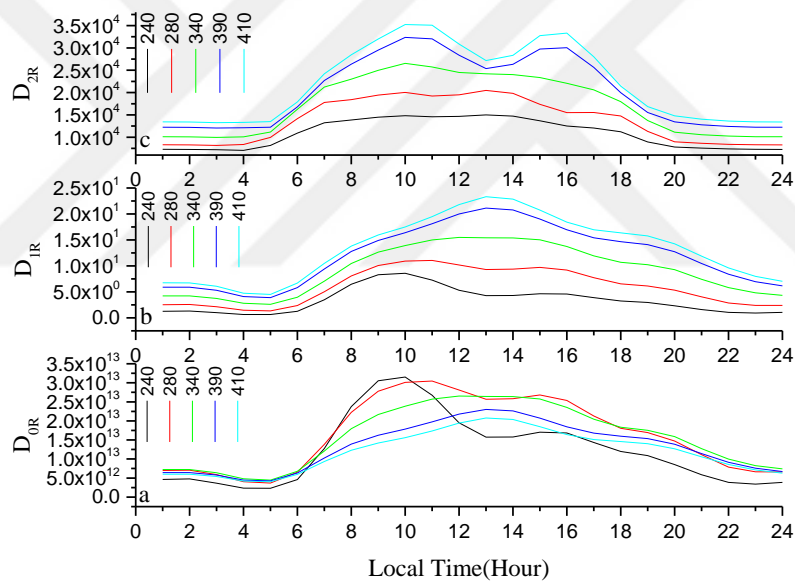


Figure 6.11. a, b, c: The Change of real part of electron diffusion coefficients by local time (December 21, $Z \neq 0$)

The change of imaginary part of electron diffusion coefficient in the ionospheric F region with local time at position of $z \neq 0$, on December 21, in the Figure 6.12. a, b, c. is seen. According to these figures, tensor elements (for 240, 280, 340, 390 and 410 km altitude) of electron diffusion coefficient show a different behavior compared to other seasons. Tensor elements of electron diffusion coefficient takes maximum value at approximately 10.00 LT and 16.00 LT. The tensor elements suddenly drop at approximately 13.00 LT. For all seasons, the tensor elements of electron diffusion coefficient in the ionospheric F region take approximately a value of (10^{17}) for figure (a) $D_{0I}(\text{m}^2/\text{sn})$ and (10^4) for figure (b) $D_{II}(\text{m}^2/\text{sn})$ while the tensor elements take approximately a value of (10^1) for (c) $D_{2I}(\text{m}^2/\text{sn})$.

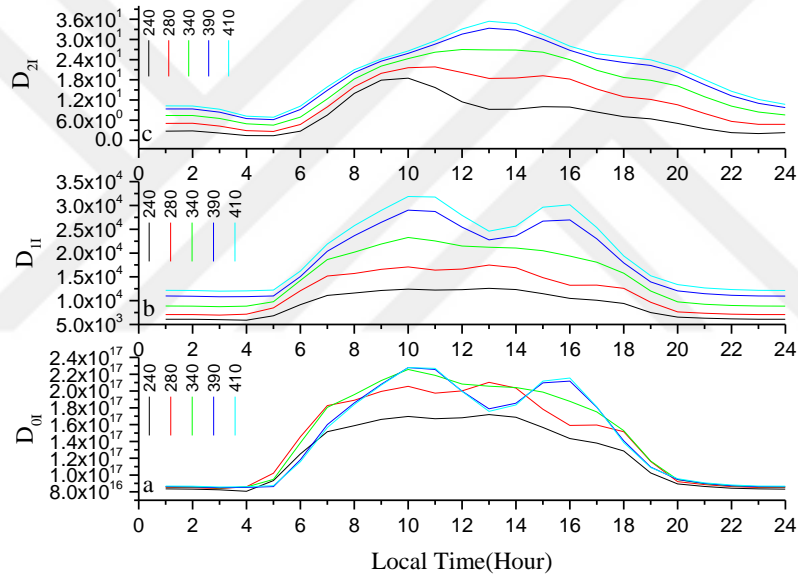


Figure 6. 12. a, b, c: The Change of electron diffusion coefficients by local time (December 21, $Z \neq 0$)

All tensor elements decrease rapidly and approximately exponentially between two maximum values in March 21, June 21 and September 23. However, in December 21, tensor elements of electron diffusion coefficient show a different behaviour compared to other seasons. tensor elements suddenly drop at approximately 13.00LT. For all seasons, tensor elements of electron diffusion coefficient in the F region of Ionosphere take approximately a value of (10^8) for figure (a) $D_0(\text{m}^2/\text{sn})$ and (10^{-1}) for figure (b) $D_1(\text{m}^2/\text{sn})$ so tensor elements of electron diffusion coefficient in the F region of Ionosphere take approximately a value of (10^3) for figure (c) $D_2(\text{m}^2/\text{sn})$.



7. CONCLUSION

This thesis has reviewed the difference of classical diffusion tensor for electrons in the low-latitude ionospheric plasma and investigated whether there were any relationships between the diffusion and equatorial anomaly. According to the findings of previous studies, the magnitude order of diffusion coefficients is approximately the same at the considered conditions (10^{10} [m^2/s]). But the difference of this thesis is that when $\omega \neq 0$, the diffusion coefficients have a real part and an imaginary structure. The imaginary part of the diffusion coefficients may give rise to the missing of the electron energy; and it is possible that this loss causes decrease in the electrical conductivity. Due to this, all of the diffusion coefficients are interpreted in terms of the electrical conductivities and motilities. This paper gives some clues of the information on the diffusion in the ionospheric plasma, how much the electromagnetic waves have influences at various frequencies sent from the ground to the ionosphere.

The findings indicate that the magnitudes of D_0 , D_1 and D_2 have bigger values calculated at 24.00 LT than 12.00 LT for both equinox and solstice days. The values of D_0 , D_1 and D_2 value calculated at both 12.00 and 24.00 LT is in the following order 10^{10} [m^2/s], $10^4 - 10^6$ (m^2/s), $10^4 - 10^6$ [m^2/s] for all seasons (March 21, June 21, September 23 and December 21), respectively. Finally, the magnitudes of the difference of the classical diffusion tensor for electrons are $D_0 > D_1 > D_2$ at Equatorial F-region for all seasons with respect to both 12.00 LT and 24.00 LT, respectively. However, D_1 and D_2 are bigger during nighttime than in the daytime, and show a behavior unlike the change with the latitude of the electron density in the magnetic equator. It is possible to say that the behavior of these abnormalities may result from electromagnetic drift and dynamo effect. The difference of classical diffusion tensor depends only on the temperature of the electron and collisions frequency of the electron D_0 in Eq.(2.4). However, the other difference diffusion, such as D_1 and D_2 are affected by the Earth's magnetic field as well as the electron temperature and electron collisions.

8. REFERENCES

- [1] Hunsucker, R.D. and Hargreaves, J., K., 2003, The High-Latitude Ionosphere and its Effects on Radio Propagation, **Cambridge University Press**, 1-50
- [2] Aydođdu M, Yeşil A, ve Güzel E, 2003, The Group Refractive Indices of HF Waves in the Ionosphere and Departure From the Magnitude Without Collisions, Elazığ,
- [3] Özcan, O., Aydođdu, M., Yeşil, A., Güzel, E., 1996, The Damping of Radio Waves in the Ionospheric Plasma over Elazığ, **F. Ü. Fen ve Müh. Bilimleri Dergisi**, s. 113–123
- [4] Rishbeth, Henry, 1973, Physics and Chemistry of the Ionospheric Contemp, **Phys**, 14,229, 240
- [5] Özcan, O, 1987, Elazığ üzerindeki iyon kürenin incelenmesi, **Yüksek Lisans Tezi, F.Ü. Fen Bilimleri Enstitüsü**, Elazığ, 11-15
- [6] Aydođdu, M., 1988, Dip Ekvatoru Üzerindeki İyon kürenin F-Bölgesindeki Elektron Kayıp Katsayısının (β) Hesaplanması, **Doğa**, **12**, 14-21
- [7] Rishbeth, H. ve Garriot, O.K. 1969, *Introduction to Ionospheric Physics*, **Academic Pres, New York**
- [8] Aydođdu, M., 1980, Ariel 4 uydusuyla elde edilen elektron yoğunluğu verilerinin 70°-80° D ve 60°-70° B boylamları arasında incelenmesi, **Doktora Tezi, E.Ü. Fen Fakültesi**, İzmir, 10-41
- [9] Karatay, S., 2005, İyon kürenin Plazmasında Kış Anormalliđi, **Yüksek Lisans Tezi, F.Ü. Fen Bilimleri Enstitüsü**, Elazığ, 10-12
- [10] Abur-Robb, M. F. K. 1969, Combined World-Wide Neutral Air Wind And Electrodynamic On The F2-Layer, Planet **Space Sci.** , **17**, 1269-1279
- [11] Bailey, G. J. Su, Y. Z. and Oyama, K.-I. 2000, Yearly Variations In The Low-Latitude Topside Ionosphere, **Ann. Geophysicae**, **18**, 789-798
- [12] Rishbeth, H. 1967, A Review of Ionospheric F Region Theory, **Proceedings of TheIee**, **55**, 16-35

- [13] Zhang, S. R., Oliver, W. L., Fukao, S. And Otsuka, Y., 2000, A Study of The Forenoon Ionospheric F2-Layer Behavior Over The Middle And Upper Atmospheric Radar, **Journal of Geophysical Research**, **105**, 15,823-15,833
- [14] Millward, G. H., Rishbeth, H., Fuller-Rowell, T. J., Aylward, A. D., Quegan, S. And Moffett, R. J., 1996, Ionospheric F2-Layer Seasonal, **Journal of Geophysical Research**, **101**, 5149-5156
- [15] Rapoport, Z. Ts. And Sinel'nikov, V. M. 1998, Experimental Electron Concentration Profiles Of The Midlatitude Lower Ionosphere, **International Journal of Geomagnetism and Aeronomy**, **1**, 2-7
- [16] Chien-Chih Lee, Bodo W. Reinisch, Quiet-Condition hmF₂, NmF₂, and B₀ variations at Jicamarca and comparison with IRI-2001 during solar maximum, **Journal of Atmospheric and Solar-Terrestrial Physics**, **68**, 2138-2146
- [17] Bittencourt. J. A. 1995, Fundamentals of plasma physics, Sao Jose dos Campos, SP, Brazil
- [18] Schunk, R.; Nagy, A. Ionospheres: physics, plasma physics, and chemistry. *Cambridge university press*. 2009; 150-200.
- [19] Maurice J-PST; Schunk R. W. Diffusion and heat flow equations for the mid-latitude topside ionosphere. **Planet. Space Sci.** 1977; 25, 907-920.
- [20] Sagir, S.; Yesil, A.; Sanac, G.; Unal, I. The characterization of diffusion tensor for mid-latitude ionospheric plasma. **Annals of Geophysics**. 2014; 57(2), A0216.
- [21] Mange P. The distribution of minor ions in electrostatic equilibrium in the high atmosphere. **J. Geophys. Res.** 1960; 65, 3833.
- [22] Schunk R. W.; Walker J. C. G. Thermal diffusion in the F2 region of ionosphere. **Planet. Space Sci.** 1970; 18, 535-557.
- [23] Bauer S. J., The structure of the topside ionosphere, **Journal of Atmospheric Science**. 1962; 12, 276-279.
- [24] Evans J. V.; Julian R. F.; Reid W. A. Incoherent scatter measurements of F-region density, temperatures and vertical velocity at Millstone Hill. M.I.T. Lincoln Lab. Rep., 1970; 477.

- [25] Zhilinskii A. P.; Tsensin L.D. Collisional diffusion of a partly-ionized plasma in magnetic field, **Sov. Phys. Uspekhi**, 1980; 131, 343-385.
- [26] Rishbeth H. The ionospheric E-layer and F-layer dynamos - a tutorial review. **J. Atmos. Sol.-Terr. Phys.**, 1997; 1873-1880.
- [27] Rishbeth H., On the theory of diffusion in the ionosphere. **Geophys. J.R. Astr. Soc.**, 1975; 41, 311-317.



CIRRICULUM VITAE

Bland Hasan Mohammednajem TALABANI

Personal Information:

Birth Date : 26.06.1988
Birth Place : Iraq
Nationality : Iraq
Marital Status : Marriage

